HHS Public Access

Author manuscript

Methods Enzymol. Author manuscript; available in PMC 2016 February 26.

Published in final edited form as:

Methods Enzymol. 2008 ; 449: 73–95. doi:10.1016/S0076-6879(08)02404-X.

Evaluating the control of mRNA decay in fission yeast

Brandon J. Cuthbertson[*] and **Perry J. Blackshear**[*,†]

[*]Laboratory of Signal Transduction, National Institute of Environmental Health Sciences, Research Triangle Park, NC 27709

[†]Clinical Research Program, National Institute of Environmental Health Sciences, Research Triangle Park, NC 27709

Abstract

Abnormalities in rates of mRNA decay can lead to changes in normal, steady-state levels of transcripts, which in turn can result in changes in protein production and abnormal phenotypes. For example, mice deficient in the gene encoding tristetraprolin (TTP), a tandem CCCH zinc finger domain protein, develop a complex syndrome that includes wasting, arthritis, and myeloid hyperplasia, all secondary to elevated levels of tumor necrosis factor alpha (TNF). This in turn reflects elevated levels of TNF mRNA, which is a direct "target" of TTP binding and TTP-promoted deadenylation and decay. Three TTP-like proteins are expressed in man, and four in mice, all of which share functional homologies of mRNA binding ability and control of transcript decay. In contrast, the *Schizosaccharomyes pombe* genome contains only one TTP-like protein, named zfs1. Microarray analysis revealed that *S. pombe* cells deficient in zfs1 overexpress the *arz1* mRNA, which has several ideal TTP-like binding sites in its 3'-untranslated region (UTR). We used the "no message in thiamine (*nmt*)" repressible system, in which thiamine rapidly shuts off gene transcription, to evaluate the relative stability of the *arz1* mRNA in wild-type and zfs1-deficient cells. We found that the *arz1* mRNA decayed much more rapidly in the presence of endogenous zfs1 than in its absence. The *nmt* system also proved useful for the study of mRNA sequence elements that are essential for interactions with zfs1, which eventually results in accelerated transcript decay. These studies illustrates the utility of the *S. pombe nmt* system for evaluating protein-mRNA interactions that affect mRNA decay *in vivo*, and provide an alternative to the use of transcription inhibitors or heat-sensitive polymerase promoters that are more commonly used to evaluate mRNA decay in *Saccharomyces cerevesiae*. We hope to use this convenient experimental system to unravel the mechanism by which TTP family members, in this and other organisms, bind to mRNAs and promote their instability.

Introduction

Control of mRNA decay is an essential phase of regulating the expression of genes into biologically active protein. Their labile nature alone is insufficient to control the timing of protein expression termination; instead, their lability is governed by the interplay among a variety of proteins. The importance of tight control of gene expression at the post-

Address correspondence to: Perry J. Blackshear, NIEHS, 111 TW Alexander Drive, MD A2-05, Research Triangle Park, NC, 27709., Tel. 919-541-4899, Fax. 919-541-4571, black009@niehs.nih.gov.

transcriptional level is particularly evident in the case of tristetraprolin (TTP), a CCCH type tandem zinc finger (TZF) domain protein. TTP is a protein encoded by *Zfp36* in mice whose absence results in a severe autoimmune and inflammatory syndrome (Lai et al., 1998; Taylor et al., 1996). TTP deficiency is associated with tumor necrosis factor-alpha (TNFα) over-expression (Blackshear, 2002; Carballo et al., 1998; Lai et al., 1998), and TTP has been shown to promote deadenylation and destruction of TNFα mRNA (Carballo et al., 1998; Lai et al., 1999). TTP may regulate overlapping aspects of immune cell function, inflammation and autoimmunity by targeting, in addition to TNFα, other essential mRNAs (Carballo et al., 1998; Carballo et al., 2000; Lai et al., 2006; Ogilvie et al., 2005).

TTP and its family members specifically bind to Adenylate Uridylate (AU)-rich elements (AREs) present in the 3'-untranslated region (3'-UTR) of select mRNAs through the TZF domain. The optimal binding site recognized by TTP and its relatives is the UUAUUUAUU nonamer (Blackshear et al., 2003; Brewer et al., 2006; Brewer et al., 2004; Hall, 2005; Hudson et al., 2004; Lai and Blackshear, 2001; Lai et al., 1999; Lai et al., 2005; Worthington et al., 2002), which is present in tandem and often overlapping repeats in TNFα, GM-CSF, and IL-2 mRNAs, each confirmed physiological targets of TTP (Carballo et al., 1998; Carballo et al., 2000; Ogilvie et al., 2005). TTP binds to and subsequently destabilizes target mRNAs by an incompletely understood mechanism that most likely involves the recruitment or activation of poly-A ribonuclease (PARN), an enzyme with 3'-5' poly(A) tail exonuclease activity (Lai et al., 2003).

CCCH TZF domain proteins are widespread in eukaryotes, with many species expressing multiple representatives of this family (Blackshear, 2002). In man, three genes encoding TTP family proteins are expressed: *ZFP36* (encoding TTP), *ZFP36L1* and *ZFP36L2*, with expression levels varying widely in different tissues (Carrick and Blackshear, 2007). At the same time, each family member retains the canonical TTP-like activity of mRNA binding and destabilization. Even the budding yeast, *Saccharomyces cerevisiae*, expresses two different TZF domain proteins, one of which (CTH2) mediates mRNA decay in response to iron deficiency (Puig et al., 2005; Thompson et al., 1996), and a second one (CTH1) whose activity has not been fully characterized. These examples illustrate the potential difficulties of studying TZF domain family proteins in species where the potential exists for biological redundancy. In contrast, the fission yeast *Schizosaccharomyces pombe* expresses only a single CCCH TZF domain protein, zfs1, with TTP-like defining characteristics; in particular, specific TZF domain residues and intra and inter-finger spacing are highly conserved between *S. pombe* and other eukaryotes (Fig. 1). We have recently found that zfs1 mirrors TTP function in that it binds to and promotes the decay of specific target mRNAs (Cuthbertson et al., 2007), as described in detail below.

Studying mRNA decay in yeasts

In general, yeast systems have proven adaptable to studies of mRNA decay, and the extensive work done in *Saccharomyces cerevisiae* is highlighted in other chapters of this volume. The mechanisms through which mRNAs are degraded in yeasts have been reviewed (Amrani et al., 2006; Coller and Parker, 2004; Garneau et al., 2007). A genome wide scan of mRNA decay that used various methods of inhibiting transcription in *S. cerevisiae*,

including temperature-sensitive mutants of yeast RNA polymerase II and chemical inhibitors of transcription such as phenanthroline and thiolutin, has been published (Grigull et al., 2004). Much less is known about the utility of such methods in *S. pombe*, although some studies using phenanthroline have provided evidence for inhibition of transcription (Kim et al., 2000; Kim et al., 2002). The utility of such chemical inhibitors in yeasts is somewhat limited, since a wide range of "off-target" effects may be observed that include increases in the expression of certain genes (Grigull et al., 2004) and stimulation of the stress transcriptional response (Adams and Gross, 1991). In *S. pombe*, temperature sensitive mutants of RNA polymerase II have been described (Mitobe et al., 2001; Mitobe et al., 1999), but studies of mRNA decay in these mutant strains have not yet been published, to our knowledge. Again heat and other stresses on yeast cells can cause dramatic changes in the levels of some mRNAs (Herruer et al., 1988; Li et al., 1999). A further confounder is that, in *S. pombe*, a subunit of RNA polymerase II (Rpb7p) is not only involved in transcription, but also appears to be involved in mRNA decay (Lotan et al., 2007). Finally, the *S. pombe nmt* (no message with thiamine) expression system has been used to a limited extent for examining mRNA decay, and we describe in detail how we have used this system below.

Systems for studying TZF protein-mediated mRNA decay

A valuable resource for evaluating the effects of deficient TTP-mediated mRNA decay has been the TTP knockout mouse model (Carballo et al., 1998; Taylor et al., 1996) and cells derived from these mice. Mice deficient in either Zfp36l1 and Zfp36l2 have also been generated (Stumpo et al., 2004). Studies in intact mice generally do not provide a direct setting in which decay can be evaluated; only the net results of inhibiting mRNA decay can be observed, exemplified by the syndrome of TNF excess in the TTP knockout mice.

Cells derived from TTP knockout mice have been used extensively for the validation of TTP target mRNAs and in studies focused on the examination of the mechanism of action of TTP-mediated mRNA decay (Carballo et al., 1998; Carballo et al., 2000; Lai et al., 2006). Cells deficient in TTP can be compared directly with normal cells, preferably derived from animals from the same litter, by northern analysis after actinomycin D (Act D) treatment (to halt transcription) in order to measure decay of target mRNAs. For example, TNFα mRNA levels were evaluated in mouse macrophages from wild-type and TTP-knockout individuals after lipopolysaccharide (LPS) treatment, followed by Act D addition (Carballo et al., 1998). A similar approach was used to demonstrate that GM-CSF mRNA is a physiological target of TTP; this study also provided evidence for an effect of TTP on mRNA deadenylation (Carballo et al., 2000). Other TTP targets, such as IL-2 (Ogilvie et al., 2005)and Ier3 (Lai et al., 2006) mRNAs, have been validated as endogenous targets using TTP-knockout fibroblasts or lymphocytes after Act D treatment.

Transcriptional repression by Act D has proved effective in many cell types, but some cell types, including macrophages, are very sensitive to the toxic properties of Act D (Lewis et al., 1995). Furthermore, Act D induces TNFα production in cultured macrophages (Wheeler et al., 1991). Act D works by binding to DNA and inhibiting gene expression, but the effects of is interaction with DNA have long been known to include cell death in certain

circumstances (Elkind et al., 1969). An alternative system for repressing transcription in mammalian cells involves using tetracycline-responsive promoters from bacteria (Gossen et al., 1995). Such an approach has recently been used in studies of mRNA decay in mammalian cells (Chen et al., 2007; Ezzeddine et al., 2007). This type of tetracycline-based control of gene expression in mammals provides several advantages in many experimental situations (Damke et al., 1995; Gossen and Bujard, 1992; Kirchhoff et al., 1995). However, the efficiency of the "tet-off" approach has been questioned due to potential issues relating to cell-specific effectiveness (Gossen and Bujard, 1995), potential transcriptional leakage (Phillips et al., 2007) and the need for repeated application of the tet-family ligands (Milo-Landesman et al., 2001).

Other studies of TTP-ARE interactions have relied on the use of transient transfection of plasmids expressing both TTP and its native or artificially constructed mRNA targets, often in cells lacking TTP, such as HEK293 cells (Lai et al., 2002). Effects of introduced TTP and its family members can be asessed in such experiments, but TTP-like proteins can not only promote the destruction of mRNAs containing optimal target sequences that are not physiological targets; they can also promote the destruction of mRNA targets containing suboptimal target sequences. In both cases, this can occur when the protein:target RNA ratios are unphysiologically high, presumably as a result of mass action and low affinity interactions. Thus, these co-transfection methods are not as reliable as the "gold standard" of using cells deficient or not in endogenous TTP and its targets. The fission yeast *S. pombe* is a system in which the single expressed TTP-like protein can be studied at native expression levels, using both endogenous target mRNA measurements as well as measurements of artificially introduced RNA after transcription shutoff using the *nmt* expression system.

Characterization of zfs1 as a mediator of mRNA decay

Gene-targeting elimination of the *zfs1* gene in *S. pombe* produces cells that do not respond to mating pheromone properly, and do not sporulate efficiently (Kanoh et al., 1995). The vegetative growth rate of *zfs1*-deficient *S. pombe* is reduced, along with cell size (Kanoh et al., 1995). Not only does zfs1 appear to play an indirect role in the regulation of pheromone signal transduction, it also appears to be required for the proper coordination of cell division, because in *zfs1*-deficient cells the formation of the division septum is not properly coordinated with the progression of mitosis (Beltraminelli et al., 1999).

No biochemical function was assigned to the zfs1 protein in these studies, but its TZF domain was clearly related to those of TTP and its family members (Fig. 1). We hypothesized that zfs1, through its TZF domain, was capable of binding to TTP-like ARE binding sequences; we therefore decided to investigate a potential role for zfs1 as a mediator of mRNA stability. Using a matched pair of zfs1-deficient and wild-type *S. pombe* strains (Beltraminelli et al., 1999), we undertook a side-by-side microarray comparison of steady state gene expression in the two strains (Cuthbertson et al., 2007). Of 123 transcripts elevated ≥1.5 fold in the zfs1-deficient cells, 12 contained apparent TTP-like ARE binding sites. The most elevated transcript that contained ideal TTP binding sites (i.e. UUAUUUAUU) was encoded by the SPCC1494.03 gene. Northern analysis confirmed that steady state levels of this transcript were elevated approximately 3.6-fold in the zfs1-

deficient cells (Figure 2). The transcript encoded by the SPCC1494.03 gene was named *arz1*, for armadillo-repeat-containing zfs1 target 1, based on the fact that the arz1 protein encoded by the SPCC1494.03 gene contains multiple armadillo-repeats, and on evidence for *arz1* mRNA targeting and decay regulation by zfs1. The evidence supporting *arz1* mRNA as a physiological target of zfs1, and the biological function of zfs1 as a mediator of mRNA decay, identified a useful system for the evaluation of mRNA decay as mediated by TZF domain proteins.

Use of the *nmt* expression system to evaluate zfs1-mediated mRNA decay

nmt

The *nmt* (no message with thiamine) expression system is constitutive (Figure 3) and, as the name indicates, thiamine repressible (Maundrell, 1993). Maximum expression from the *nmt* promoter is achieved after 18 hr of growth in normal medium containing thiamine (Maundrell, 1990; Maundrell, 1993). We used a commercially available version of the *nmt* promoter-based expression vector (Invitrogen, Carlsbad, CA) that has a mutated TATA box, which reduces expression levels to ~15% of the unmodified *nmt* promoter (Basi et al., 1993); various other versions of the *nmt* vector, with different promoter strengths, are also available. The *nmt* expression system has been used to examine mRNA decay in *S. pombe* (Daga et al., 2003), and appeared to be an attractive alternative to other approaches for inhibiting transcription in yeast (Adams and Gross, 1991; Grigull et al., 2004; Herruer et al., 1988; Kim et al., 2002; Li et al., 1999) for many reasons, including the rapid nature of transcription repression and the ability to avoid stressful conditions that alter the levels of many mRNAs (Adams and Gross, 1991; Herruer et al., 1988; Li et al., 1999).

The nmt/arz1 expression construct

For our studies, genomic DNA from *S. pombe* was used as a template for PCR amplification of the SPCC1494.03 open reading frame (ORF) plus 1 kb of downstream genomic sequence predicted to include the complete *arz1* coding region and 3'-UTR. About half of *S. pombe* genes are intron-free, including SPCC1494.03, often permitting the use of genomic DNA in expression vector construction. A high fidelity polymerase mix, Platinum Taq Polymerase High Fidelity (Invitrogen, Carlsbad, CA), was used for the *arz1* amplification, using arz1 gene specific primers F1 and R1 (Table I), following the manufacturer's protocol for a 2.5 kbp product. The *arz1* PCR product (2,478 bp) was cloned into the TOPO TA pNMT41 system (Invitrogen, Carlsbad, CA) and transformed into ultracompetent *E. coli*, provided with the TOPO kit, which were plated on LB plates supplemented with 100 μg/ml ampicillin. Colonies were grown overnight in selective medium, and *nmt/arz1* plasmids were purified using a standard Qiagen (Valencia, CA) miniprep kit following the manufacturer's protocol. Plasmid DNA yield was checked spectrophotometrically, and by agarose gel electrophoresis and ethidium bromide staining followed by ultra-violet light visualization in preparation for plasmid DNA digestion with the restriction endonuclease EcoR1. This excised the *arz1* insert from the vector in two pieces (fragments of 333 bp and 2161 bp) due to the presence of an internal EcoR1 site. DNA sequencing of the plasmids confirmed the proper insertion and orientation of *arz1* for expression in *S. pombe*. The wild-type *S. pombe* strain used in our studies has a *leu1* mutation (*leu1-32*) that confers leucine

auxotrophy; this was the background strain for the zfs1-deficient strain that was generated through gene targeted replacement of the *zfs1* gene (Beltraminelli et al., 1999). The *nmt/arz1* expression construct contains a cassette that confers leucine prototrophy. Wild-type and zfs1-deficient *S. pombe* leu auxotrophic strains were transformed with the *nmt/arz1* expression construct following a standard chemical/heat shock method (Bahler et al., 1998). Both strains were grown on Yeast Extract Supplemented (YES) agar at 30 °C in preparation for liquid culture. Single colonies of each strain from fresh plates were used to inoculate 25 ml cultures in Edinburg Minimal Medium (EMM) supplemented with 50 mg/l each of adenine, histidine, leucine, lysine and uracil (EMM+5S) in 125 ml Belco (Vineland, NJ) glass culture flasks. Cultures were grown at 30 °C (shaking at 200 rpm) well into logarithmic growth phase until a 1:10 dilution of culture in fresh medium yielded A_{600} ≥1.0 after 3–4 days. An aliquot of each starter culture (20 ml) was then added to 80 ml of fresh EMM+5S in 500 ml Belco glass culture flasks and grown for 5 hr at 30 °C with shaking at 200 rpm to ensure that newly divided cells were present in culture for transformation. Cells were then pelleted by centrifugation at 2,000 × g for 5 min at room temperature (RT), washed with an equal volume of autoclaved water at RT and collected again by centrifugation. The cell pellets were resuspended in 1 ml of autoclaved water at RT and transferred to 1.5 ml tubes. Cells were again collected by centrifugation (2,000 × g for 5 min at RT) in a microcentrifuge and washed with 1 ml of 1 X lithium acetate (LiAc)/tris-EDTA (TE). For 10 X LiAc, 1 M lithium acetate was adjusted to pH 7.5 with diluted acetic acid. For 10 X TE, 0.1 M Tris-HCl, 0.01 M EDTA at pH 7.5 was used (Bahler et al., 1998). Cell pellet volume was then estimated (at ~200 μl) by comparing with known volumes of water in separate tubes. An equal volume of 1 × LiAc/TE was then used to resuspend the cells to achieve a concentrated solution in preparation for transformation.

S. pombe nmt/arz1 transformants

For each strain, 100 μl of the concentrated cell suspension was added to a new 1.5 ml tube containing 20 μg of sheared salmon sperm DNA in 4 μl of water and 3 μg of *nmt/arz1* plasmid DNA in10 μl of water, gently mixed and incubated at RT for 10 min. Next, 260 μl of 40% polyethylene glycol 3550 (PEG 3550) in 1 X LiAc/TE was added, and the suspension was gently mixed and incubated at 30 °C for 1 hr. For 10 ml of 40% PEG in 1 X LiAc/TE, 4 g of PEG 3550 was added to 1 ml of 10 X LiAc and 1ml of 10 X TE with 4.54 ml of water in a small beaker and mixed with a small stir bar. The mixture was then sterile filtered through a 0.2 micron syringe filter (Millipore, Billerica, MA). Dimethylsulfoxide (43 μl) was added, and the suspension was mixed gently and heated at 42 °C for 5 min in a water bath. Cells were then collected by centrifugation (2,000 × g for 5 min at RT) in a microcentrifuge. The cell pellet was observed to be slightly translucent after PEG treatment. The cell pellet was then washed with 0.5 ml of water, cells were collected again and resuspended in 0.5 ml of water and the suspension was plated on EMM supplemented with 50 mg/l of adenine, histidine, lysine and uracil (EMM+4S-Leu) using autoclaved, dried glass beads, and grown at 30 °C for 5 days. (Note: sterile technique should be used throughout the yeast transformation procedure to prevent contamination by airborne fungi. The use of sterile autoclaved water for making transformation reagents and for cell washing is essential.) Leu prototrophic colonies were streaked for isolation on fresh EMM+4S-Leu plates, and grown at 30 °C for 3 days.

Colonies confirmed for Leu prototrophy were screened by colony PCR for the presence of the *nmt/arz1* plasmid. Colony PCR was carried out as follows using BioLine Taq Polymerase (Medicorp, Montréal, Québec, Canada) in a standard PCR reaction mixture based on the manufacturer's protocol that included an *nmt* vector-specific 5' PCR primer (the *nmt* forward primer, listed in Table I) and an *arz1* internal 3' PCR primer (F2 and R2). The reaction mixture was kept on ice and inoculated with a small volume of cells from a Leu prototrophic colony. Briefly, a single colony was touched with the end of a small volume pipet tip such that a visible amount of cells was present on the end of the tip, and the cells were applied to the PCR reaction mix, resulting in a visibly turbid mixture. Variation from semi-translucent to nearly opaque mixtures did not appear to affect PCR results substantially, and it was important to deliver enough cells to provide sufficient template for gene amplification. Once cells were suspended in the PCR reaction mixture, it was heated at 94 °C for 5 min in the thermocycler to ensure yeast cell wall lysis, and kept at 4 °C while the Taq polymerase was added. A negative control sample was generated from a colony of wild-type *S. pombe*, and a positive control included 30 ng of purified *nmt/arz1* plasmid. Amplification proceeded for 40 cycles in order to produce sufficient product (374 bp) for visualization by agarose gel electrophoresis and ethidium bromide staining. Clones that were confirmed to be PCR positive for the *nmt/arz1* expression construct were maintained on EMM+4S-Leu plates and restreaked weekly when cultures were being analyzed for expression.

Repression of arz1 transcription with thiamine

Individual colonies of wild-type and zfs1-deficient *S. pombe* transformed with the *nmt/arz1* construct (named W1 and Z1, respectively) were grown in sterile filtered EMM+4S-Leu broth at 30 °C with shaking at 200 rpm, well into logarithmic growth phase, at which time (about 3–4 days) a 1:10 dilution of culture in fresh media read ≥1.0 A_{600}, in order to ensure that the *nmt*-driven expression was maximal. Replicate cultures derived from separate colonies grown under identical conditions (five for each strain) were used for statistical analysis of the data. Starter cultures (in 30 ml of EMM+4S-Leu) were diluted to 0.7–0.8 A_{600} in 30 ml of fresh medium and grown for 4 hr at 30 °C with shaking at 200 rpm in preparation for time course studies. Five replicates each of W1 and Z1 paired cultures were cultured and compared directly in the following assay. For each experimental replicate, W1 and Z1 cultures were removed from the 30 °C shaker and 1.5 ml of each culture was transferred to a 1.5 ml microcentrifuge tube. Cells were pelleted by centrifugation at maximum speed (approximately 17,000 × g) in a microcentrifuge for 1 min, and the supernatant was removed using a vacuum aspirator. The W1 and Z1 cell pellets were simultaneously snap frozen in liquid nitrogen, and thiamine was immediately added to the cultures to a final concentration of 10 μM (28.5 μl from a 10 mM stock solution in water) as the time course was started, and cultures were returned to the 30 °C shaker. The pre-thiamine treatment cell pellets were considered to be time zero samples. After 7.5 min, thiamine-treated W1 and Z1 cultures were removed and sampled in an identical manner, so that cell pellets were snap-frozen by 10 min. Time course sampling proceeded until 20 min and 40 min samples were collected. Cell pellets were then stored at −80 °C until total RNA could be isolated.

Total RNA isolation

Total RNA was prepared from cell pellets using the MasterPure Yeast RNA purification kit (Epicentre, Madison, WI). For this isolation, frozen cell pellets were placed on ice, and 300 μl of Extraction Reagent supplemented with proteinase K (0.17 μg/μl final concentration) was added to each sample. Pellets were resuspended by vortexing, and samples were incubated at 70 °C for 15 min with vortexing every 5 min. Samples were then placed on ice for 5 min and 175 μl of (MCP) protein precipitation reagent was added, followed by vigorous vortexing for 10 sec. The precipitate was pelleted by centrifugation at 14,000 × g at 4 °C for 30 min. Shorter centrifugation times are recommended by the manufacturer's protocol, but we recommend extended spins at higher speeds to prevent debris carryover into the precipitation steps. During the centrifugation step, 0.5 ml of isopropanol was added to RNase/DNase-free 1.5 ml tubes. Supernatants were added to the isopropanol-containing tubes at RT in order to precipitate RNA, and the tubes were mixed by inversion 40 times. Inversion can be done quickly by holding the 1.5 ml tubes between two standard tube racks. Total RNA was then collected by centrifugation at 14,000 × g at 4 °C for 30 min and then kept on ice. Supernatants were removed carefully so that the pellets were not aspirated, which may occur if a vacuum aspirator is used or if the pellets are kept on ice for an extended time. RNA pellets were washed with 0.5 ml of 70% ethanol and centrifuged at 14,000 × g at 4 °C for 5 min. The wash supernatants were carefully removed by pipetting; residual ethanol was collected in the bottom of the tube (20–50 μl) with another brief centrifuge spin and was removed by pipetting. The manufacturer's protocol suggests multiple ethanol wash steps, but we found that one wash was sufficient for obtaining RNA of suitable quantity and quality for northern analysis. Pellets were resuspended in deionized, double autoclaved water supplemented with ribonuclease inhibitor (Invitrogen, Carlsbad, Ca, to final concentration 10 μl/ml) by vortexing vigorously. Total RNA concentrations were calculated based on A_{260}, and 10 μg of total RNA from each sample was transferred to a RNase/DNase free 1.5 ml tube and lyophilized in a speed vac at RT. Remaining RNA and dried samples were stored at −80 °C.

Northern analysis and transcript quantitation

Denaturing gel electrophoresis

Lyophilized total RNA isolated from wild-type and zfs1-deficient strains, and from each of these strains transformed with the *nmt/arz1* construct (W1 and Z1, respectively), was resuspended in 8.8 μl of denaturing solution per sample by incubation at 70 °C for 6 min in a dry bath with brief vortexing at 3 min. Denaturing solution consisted of 2 μl of water, 0.88 μl of autoclaved 10 X MOPS buffer (pH 7.0), 1.56 μl of formaldehyde and 4.44 μl of deionized formamide per 8.8 μl of total volume. Resuspended samples were held on ice for 1 min, and 4.5 μl of northern loading dye was added. The resuspended mixture was vortexed briefly and held on ice in preparation for loading. A 0.3 l, 1.2% agarose gel was prepared by dissolving 3.6 g of agarose in 217.2 ml of water in a 0.5 l bottle with a stir bar. After boiling, the dissolved gel was stirred under a fume hood while 52 ml of formaldehyde (37.5%) and 30 ml of autoclaved 10 X MOPS buffer, pH 7.0, were added. After the mixture cooled, a 20 × 25 cm gel was poured so that samples could be loaded (up to 40 per gel with 20 in each of the upper and lower halves of the gel) in large wells (8 × 1 mm) (Figure 4). Wild-type and

zfs1-deficient samples were subjected to electrophoresis on the same gel if possible (data summarized in Figure 2). Direct comparisons between samples separated on the same gel and carried through the complete analysis at the same time were used for quantitative comparisons. Gels were run in 1 X MOPS buffer for 18 hr at ~30 volts. The gels were then transferred to large (~22 × 28 cm) plastic containers and stained with 33 μg/ml acridine orange in 10 mM NaH_2PO_4, pH 6.8 for 15 min, washed twice in 10 mM NaH_2PO_4, pH 6.8 for 30 min, cut in half along the wells dividing the upper and lower sections of the gel to facilitate ease in handling, and evaluated for sample loading and ribosomal RNA migration by UV imaging.

Northern blotting

RNA from the gels was transferred to Hybond N+ nylon membranes (Amersham, Biosciences, Piscataway, NJ), pre-wetted with sterile water, using the basic capillary technique (Sambrook, 1989) overnight using 10 X SSC as the mobile phase. Membranes were gently rinsed with 10 X SSC to remove any possible debris remaining from the contact with the gel after transfer. Membranes were UV cross-linked and dried at RT between absorbent papers (Whatman 1; Whatman, Kent, UK). Membranes were pre-hybridized in 50% deionized formamide, 5 X SSC, 50 mM Na_2HPO_4 (pH 6.5), 0.5% SDS, 1 X Denhardt's solution and 150 μl/ml denatured, sheared salmon sperm DNA in water that was boiled for 5 min and cooled in order to denature the salmon sperm DNA. Prehybridization was carried out at 42 °C in a hybridization bottle overnight. An *arz1* DNA fragment (665 bp) was generated by PCR using gene specific primers F3 and R3 (Table I), and 50 ng of this fragment was labeled and used as a gene-specific probe. The *arz1* probe was random prime-labeled with a High Prime kit (Roche, Indianapolis, IN) to incorporate dCTP-α ^{32}P (Perkin Elmer, Wellesley, MA), as was an actin control probe also generated by PCR using F4 and R4 primers (Table I). Percent incorporation, ~50%, was determined after the labeled probe was separated from unincorporated isotope by desalting (G-50, Roche) by counting 1 μl each of reaction mix and desalted probe, allowing an estimation of labeling efficiency. Dextran sulphate (1 ml of a 50% (w/v) solution in water) was added to 4 ml of fresh prehybridization solution in a 15 ml polypropylene Falcon tube (BD Biosciences, San Jose, CA) and boiled for 5 min. Radiolabeled probe was then added to the hot hybridization solution, and the mixture was allowed to cool for 5 min at RT so that an excessively hot solution was not applied to the RNA blot. This was poured directly into the hybridization bottle after removal of the prehybridization solution. Hybridization occurred overnight at 42 °C. The filters were then washed once in the hybridization bottle with 20 ml of 1 × SSC, 0.1% SDS at RT, and in a plastic dish with enough 1 × SSC, 0.1% SDS at RT to cover the membrane (~150 ml) with shaking at least four times for 5 min. Two additional washes were then done in the same manner at 60 °C for 15 min each. Filters were blotted on paper towels to remove excess wash solution, wrapped in plastic wrap and exposed to phosphorimager screens for 2–3 hr. Screens were scanned using the Typhoon system and quantitation was performed using ImageQuant 5.1 (Amersham Biosciences, Piscataway, NJ).

Northern analysis results

As was the case for the endogenous *arz1* mRNA levels, the nmt-expressed *arz1* mRNA levels were consistently greater in the zfs1-deficient strain, but the overall expression levels

in both strains varied by as much as two-fold (Figure 4B). Nevertheless, the variation was minimal across independent biological replicates (Figure 4B–C). *arz1* mRNA levels at 0, 10, 20 and 40 min were corrected for endogenous levels in each strain, and corrected for loading variation by actin mRNA levels. The corrected intensities were used to compare the relative *arz1* mRNA levels after thiamine addition by dividing the intensity (volume) at 0, 10, 20 and 40 min by the intensity at 0 min, yielding a set of values that ranged from 1 (for the 0 min sample) to ~ 0.25 by 20 min. These fractions, shown as % of time 0 in Figures 4C and 5C–D, were compiled and compared in a pairwise fashion using GraphPad Prism 4 (GraphPad Software, Inc., San Diego, CA). Two tailed t-tests were used to compare mean values from the two strains at each time point.

Utility of the *S. pombe* zfs1 model

A significant difference was observed for *nmt*-expressed *arz1* mRNA levels in the two strains at the 10 min time point, but by 20 min the difference was lost. This result was consistent with *arz1* being a target of zfs1, as were results from additional studies that involved earlier time courses as well as recombinant zfs1 protein binding to an *arz1* ARE-based RNA oligonucleotide.

S. cerevisiae has been used to evaluate CCCH TZF domain protein binding to RNA, using yeast three-hybrid interaction strategies (Puig et al., 2005). In that study, mutations in CTH2 target sequences in the RNA eliminated the interaction. In contrast, we used a direct assessment of RNA decay to evaluate normal and mutated ARE binding sites in *S. pombe* arz1. Two ARE-containing areas were identified based on the presence of the optimal UUAUUUAUU binding sites for mammalian TTP family members. The *nmt/arz1* system was then used to evaluate the effect of a range of mutations in predicted binding sites on mRNA decay in the presence and absence of zfs1. Site directed mutagenesis was carried out using gene-specific primers (Table II) for the *arz1* 3'-UTR, including a pair that targeted two adjacent binding sites (AREb) for mutation (primers FMuB, RMuB). The adjacent sites at AREb appeared to be essential for zfs1-mediated decay, and no significant difference was observed when comparing means for MuB to Z1. The predicted zfs1 binding site that is more 5' does not appear to be essential for zfs1-mediated decay (Figure 5B). The differences between the WT and the mutant sequences are shown in Fig. 5C, and emphasize the similarities between *arz1* with a non-binding AREa (MuA) and the normal *arz1* sequence (W1).

As a system for studying TTP family member function, the *S. pombe* zfs1 system presents a number of advantages, including the genetic tractability of the organism, the single TTP family member expressed, the ability to use the *nmt* system to turn off selected gene transcription, and others. Time will tell whether this system will increase our understanding of the mechanism by which TTP family members promote mRNA deadenylation and decay. We now know at least one physiological target of zfs1, *arz1*, with others predicted from a microarray screen (Cuthbertson et al., 2007). The arz1 protein has not yet been functionally characterized, but its sequence resembles members of the armadillo/beta-catenin family. Neither Drosophila armadillo nor human beta-catenin encoding mRNAs contain obvious TTP-family ARE binding sites in their 3'-UTRs transcripts. Vimar, a protein encoded by a

Drosophila ORF, is the closest database hit for arz1, and contains numerous potential TTP binding sites in a 1 kb region downstream of the stop codon. Ultimately, we hope to be able to link the biochemical effects of zfs1 on mRNA turnover to its apparent physiological role in the control of a signal transduction cascade that is essential for mating in *S. pombe*. This type of physiological connection is nicely illustrated in the case of CTH2 from *S. cerevisiae*, which is an iron-regulated protein that in turn appears to regulate the stability of a group of transcripts encoding proteins involved in various aspects of iron metabolism (Puig et al., 2005). Consistent with previous observations (Mercier et al., 2006), zfs1 deficiency does not appear to affect iron metabolism (Cuthbertson et al., 2007). Our hope is that not only will the zfs1 protein be found to coordinate the stability of a similar collection of transcripts involved in an important physiological process in *S. pombe*, but that we can use this system to gain insights into the biochemical function of the whole class of CCCH tandem zinc finger proteins.

Acknowledgments

We would like to thank Debbie Stumpo for help with northern blots and helpful discussions, Yanhong Liao for help with the *S. pombe* system, and Wi Lai for insightful discussions. We also acknowledge the help of the NIEHS Microarray Core. This work was supported by the Intramural Research Program of the NIH, NIEHS.

References

Adams CC, Gross DS. The yeast heat shock response is induced by conversion of cells to spheroplasts and by potent transcriptional inhibitors. J Bacteriol. 1991; 173:7429–7435. [PubMed: 1938939]

Amrani N, Sachs MS, Jacobson A. Early nonsense: mRNA decay solves a translational problem. Nat Rev Mol Cell Biol. 2006; 7:415–425. [PubMed: 16723977]

Bahler J, Wu JQ, Longtine MS, Shah NG, McKenzie A 3rd, Steever AB, Wach A, Philippsen P, Pringle JR. Heterologous modules for efficient and versatile PCR-based gene targeting in Schizosaccharomyces pombe. Yeast. 1998; 14:943–951. [PubMed: 9717240]

Basi G, Schmid E, Maundrell K. TATA box mutations in the Schizosaccharomyces pombe nmt1 promoter affect transcription efficiency but not the transcription start point or thiamine repressibility. Gene. 1993; 123:131–136. [PubMed: 8422997]

Beltraminelli N, Murone M, Simanis V. The S. pombe zfs1 gene is required to prevent septation if mitotic progression is inhibited. J Cell Sci. 1999; 112(Pt 18):3103–3114. [PubMed: 10462526]

Blackshear PJ. Tristetraprolin and other CCCH tandem zinc-finger proteins in the regulation of mRNA turnover. Biochem Soc Trans. 2002; 30:945–952. [PubMed: 12440952]

Blackshear PJ, Lai WS, Kennington EA, Brewer G, Wilson GM, Guan X, Zhou P. Characteristics of the interaction of a synthetic human tristetraprolin tandem zinc finger peptide with AU-rich element-containing RNA substrates. J Biol Chem. 2003; 278:19947–19955. [PubMed: 12639954]

Brewer BY, Ballin JD, Fialcowitz-White EJ, Blackshear PJ, Wilson GM. Substrate dependence of conformational changes in the RNA-binding domain of tristetraprolin assessed by fluorescence spectroscopy of tryptophan mutants. Biochemistry. 2006; 45:13807–13817. [PubMed: 17105199]

Brewer BY, Malicka J, Blackshear PJ, Wilson GM. RNA sequence elements required for high affinity binding by the zinc finger domain of tristetraprolin: conformational changes coupled to the bipartite nature of Au-rich MRNA-destabilizing motifs. J Biol Chem. 2004; 279:27870–27877. [PubMed: 15117938]

Carballo E, Lai WS, Blackshear PJ. Feedback inhibition of macrophage tumor necrosis factor-alpha production by tristetraprolin. Science. 1998; 281:1001–1005. [PubMed: 9703499]

Carballo E, Lai WS, Blackshear PJ. Evidence that tristetraprolin is a physiological regulator of granulocyte-macrophage colony-stimulating factor messenger RNA deadenylation and stability. Blood. 2000; 95:1891–1899. [PubMed: 10706852]

Carrick DM, Blackshear PJ. Comparative expression of tristetraprolin (TTP) family member transcripts in normal human tissues and cancer cell lines. Arch Biochem Biophys. 2007; 462:278–285. [PubMed: 17517366]

Chen CY, Yamashita Y, Chang TC, Yamashita A, Zhu W, Zhong Z, Shyu AB. Versatile applications of transcriptional pulsing to study mRNA turnover in mammalian cells. Rna. 2007; 13:1775–1786. [PubMed: 17728382]

Coller J, Parker R. Eukaryotic mRNA decapping. Annu Rev Biochem. 2004; 73:861–890. [PubMed: 15189161]

Cuthbertson BJ, Liao Y, Birnbaumer L, Blackshear PJ. Characterization of zfs1 as an mRNA binding and destabilizing protein in Schizosaccharomyces pombe. J Biol Chem. 2007 (in press).

Daga RR, Bolanos P, Moreno S. Regulated mRNA stability of the Cdk inhibitor Rum1 links nutrient status to cell cycle progression. Curr Biol. 2003; 13:2015–2024. [PubMed: 14653990]

Damke H, Gossen M, Freundlieb S, Bujard H, Schmid SL. Tightly regulated and inducible expression of dominant interfering dynamin mutant in stably transformed HeLa cells. Methods Enzymol. 1995; 257:209–220. [PubMed: 8583923]

Elkind MM, Kano E, Sutton-Gilbert H. Cell killing by actinomycin D in relation to the growth cycle of chinese hamster cells. J Cell Biol. 1969; 42:366–377. [PubMed: 5792326]

Ezzeddine N, Chang TC, Zhu W, Yamashita A, Chen CY, Zhong Z, Yamashita Y, Zheng D, Shyu AB. Human TOB, an Antiproliferative Transcription Factor, Is a Poly(A)-Binding Protein-Dependent Positive Regulator of Cytoplasmic mRNA Deadenylation. Mol Cell Biol. 2007; 27:7791–7801. [PubMed: 17785442]

Garneau NL, Wilusz J, Wilusz CJ. The highways and byways of mRNA decay. Nat Rev Mol Cell Biol. 2007; 8:113–126. [PubMed: 17245413]

Gossen M, Bujard H. Tight control of gene expression in mammalian cells by tetracycline-responsive promoters. Proc Natl Acad Sci U S A. 1992; 89:5547–5551. [PubMed: 1319065]

Gossen M, Bujard H. Efficacy of tetracycline-controlled gene expression is influenced by cell type: commentary. Biotechniques. 1995; 19:213–216. discussion 216-7. [PubMed: 8527141]

Gossen M, Freundlieb S, Bender G, Muller G, Hillen W, Bujard H. Transcriptional activation by tetracyclines in mammalian cells. Science. 1995; 268:1766–1769. [PubMed: 7792603]

Grigull J, Mnaimneh S, Pootoolal J, Robinson MD, Hughes TR. Genome-wide analysis of mRNA stability using transcription inhibitors and microarrays reveals posttranscriptional control of ribosome biogenesis factors. Mol Cell Biol. 2004; 24:5534–5547. [PubMed: 15169913]

Hall TM. Multiple modes of RNA recognition by zinc finger proteins. Curr Opin Struct Biol. 2005; 15:367–373. [PubMed: 15963892]

Herruer MH, Mager WH, Raue HA, Vreken P, Wilms E, Planta RJ. Mild temperature shock affects transcription of yeast ribosomal protein genes as well as the stability of their mRNAs. Nucleic Acids Res. 1988; 16:7917–7929. [PubMed: 3047675]

Hudson BP, Martinez-Yamout MA, Dyson HJ, Wright PE. Recognition of the mRNA AU-rich element by the zinc finger domain of TIS11d. Nat Struct Mol Biol. 2004; 11:257–264. [PubMed: 14981510]

Kanoh J, Sugimoto A, Yamamoto M. Schizosaccharomyces pombe zfs1+ encoding a zinc-finger protein functions in the mating pheromone recognition pathway. Mol Biol Cell. 1995; 6:1185–1195. [PubMed: 8534915]

Kim M, Lee W, Park J, Kim JB, Jang YK, Seong RH, Choe SY, Park SD. The stress-activated MAP kinase Sty1/Spc1 and a 3'-regulatory element mediate UV-induced expression of the uvi15(+) gene at the post-transcriptional level. Nucleic Acids Res. 2000; 28:3392–3402. [PubMed: 10954610]

Kim MJ, Kim M, Park SD. Post-transcriptional regulation of ura4+ gene expression by glucose in Schizosaccharomyces pombe. Mol Cells. 2002; 14:437–443. [PubMed: 12521309]

Kirchhoff S, Koster M, Wirth M, Schaper F, Gossen M, Bujard H, Hauser H. Identification of mammalian cell clones exhibiting highly regulated expression from inducible promoters. Trends Genet. 1995; 11:219–220. [PubMed: 7638903]

Lai WS, Blackshear PJ. Interactions of CCCH zinc finger proteins with mRNA: tristetraprolin-mediated AU-rich element-dependent mRNA degradation can occur in the absence of a poly(A) tail. J Biol Chem. 2001; 276:23144–23154. [PubMed: 11279239]

Lai WS, Carballo E, Strum JR, Kennington EA, Phillips RS, Blackshear PJ. Evidence that tristetraprolin binds to AU-rich elements and promotes the deadenylation and destabilization of tumor necrosis factor alpha mRNA. Mol Cell Biol. 1999; 19:4311–4323. [PubMed: 10330172]

Lai WS, Carrick DM, Blackshear PJ. Influence of nonameric AU-rich tristetraprolin-binding sites on mRNA deadenylation and turnover. J Biol Chem. 2005; 280:34365–34377. [PubMed: 16061475]

Lai WS, Kennington EA, Blackshear PJ. Interactions of CCCH zinc finger proteins with mRNA: non-binding tristetraprolin mutants exert an inhibitory effect on degradation of AU-rich element-containing mRNAs. J Biol Chem. 2002; 277:9606–9613. [PubMed: 11782475]

Lai WS, Kennington EA, Blackshear PJ. Tristetraprolin and its family members can promote the cell-free deadenylation of AU-rich element-containing mRNAs by poly(A) ribonuclease. Mol Cell Biol. 2003; 23:3798–3812. [PubMed: 12748283]

Lai WS, Parker JS, Grissom SF, Stumpo DJ, Blackshear PJ. Novel mRNA targets for tristetraprolin (TTP) identified by global analysis of stabilized transcripts in TTP-deficient fibroblasts. Mol Cell Biol. 2006; 26:9196–9208. [PubMed: 17030620]

Lai WS, Thompson MJ, Blackshear PJ. Characteristics of the intron involvement in the mitogen-induced expression of Zfp-36. J Biol Chem. 1998; 273:506–517. [PubMed: 9417109]

Lewis JG, Adams DO, Fan S. Selective sensitivity of macrophages to cytotoxicity by inhibitors of macromolecular synthesis: induction of apoptosis. J Leukoc Biol. 1995; 57:635–642. [PubMed: 7536790]

Li B, Nierras CR, Warner JR. Transcriptional elements involved in the repression of ribosomal protein synthesis. Mol Cell Biol. 1999; 19:5393–5404. [PubMed: 10409730]

Lotan R, Goler-Baron V, Duek L, Haimovich G, Choder M. The Rpb7p subunit of yeast RNA polymerase II plays roles in the two major cytoplasmic mRNA decay mechanisms. J Cell Biol. 2007; 178:1133–1143. [PubMed: 17875743]

Maundrell K. nmt1 of fission yeast. A highly transcribed gene completely repressed by thiamine. J Biol Chem. 1990; 265:10857–10864. [PubMed: 2358444]

Maundrell K. Thiamine-repressible expression vectors pREP and pRIP for fission yeast. Gene. 1993; 123:127–130. [PubMed: 8422996]

Mercier A, Pelletier B, Labbe S. A transcription factor cascade involving Fep1 and the CCAAT-binding factor Php4 regulates gene expression in response to iron deficiency in the fission yeast Schizosaccharomyces pombe. Eukaryot Cell. 2006; 5:1866–1881. [PubMed: 16963626]

Milo-Landesman D, Surana M, Berkovich I, Compagni A, Christofori G, Fleischer N, Efrat S. Correction of hyperglycemia in diabetic mice transplanted with reversibly immortalized pancreatic beta cells controlled by the tet-on regulatory system. Cell Transplant. 2001; 10:645–650. [PubMed: 11714200]

Mitobe J, Mitsuzawa H, Ishihama A. Functional analysis of RNA polymerase II Rpb3 mutants of the fission yeast Schizosaccharomyces pombe. Curr Genet. 2001; 39:210–221. [PubMed: 11453250]

Mitobe J, Mitsuzawa H, Yasui K, Ishihama A. Isolation and characterization of temperature-sensitive mutations in the gene (rpb3) for subunit 3 of RNA polymerase II in the fission yeast Schizosaccharomyces pombe. Mol Gen Genet. 1999; 262:73–84. [PubMed: 10503538]

Ogilvie RL, Abelson M, Hau HH, Vlasova I, Blackshear PJ, Bohjanen PR. Tristetraprolin down-regulates IL-2 gene expression through AU-rich element-mediated mRNA decay. J Immunol. 2005; 174:953–961. [PubMed: 15634918]

Phillips JE, Gersbach CA, Garcia AJ. Virus-based gene therapy strategies for bone regeneration. Biomaterials. 2007; 28:211–229. [PubMed: 16928397]

Puig S, Askeland E, Thiele DJ. Coordinated remodeling of cellular metabolism during iron deficiency through targeted mRNA degradation. Cell. 2005; 120:99–110. [PubMed: 15652485]

Sambrook, J.; Fritsch, EFM.; Maniatis, T. “Molecular cloning: a laboratory manual.”. New York: Cold Spring Harbor Laboratory Press, Cold Spring Harbor; 1989.

Stumpo DJ, Byrd NA, Phillips RS, Ghosh S, Maronpot RR, Castranio T, Meyers EN, Mishina Y, Blackshear PJ. Chorioallantoic fusion defects and embryonic lethality resulting from disruption of

Zfp36L1, a gene encoding a CCCH tandem zinc finger protein of the Tristetraprolin family. Mol Cell Biol. 2004; 24:6445–6455. [PubMed: 15226444]

Taylor GA, Carballo E, Lee DM, Lai WS, Thompson MJ, Patel DD, Schenkman DI, Gilkeson GS, Broxmeyer HE, Haynes BF, Blackshear PJ. A pathogenetic role for TNF alpha in the syndrome of cachexia, arthritis, and autoimmunity resulting from tristetraprolin (TTP) deficiency. Immunity. 1996; 4:445–454. [PubMed: 8630730]

Thompson MJ, Lai WS, Taylor GA, Blackshear PJ. Cloning and characterization of two yeast genes encoding members of the CCCH class of zinc finger proteins: zinc finger-mediated impairment of cell growth. Gene. 1996; 174:225–233. [PubMed: 8890739]

Wheeler HR, Rockett EJ, Clark I, Geczy CL. Actinomycin D upregulates lipopolysaccharide induction of macrophage procoagulant expression and tumour necrosis factor-alpha production. Clin Exp Immunol. 1991; 86:304–310. [PubMed: 1934597]

Worthington MT, Pelo JW, Sachedina MA, Applegate JL, Arseneau KO, Pizarro TT. RNA binding properties of the AU-rich element-binding recombinant Nup475/TIS11/tristetraprolin protein. J Biol Chem. 2002; 277:48558–48564. [PubMed: 12324455]

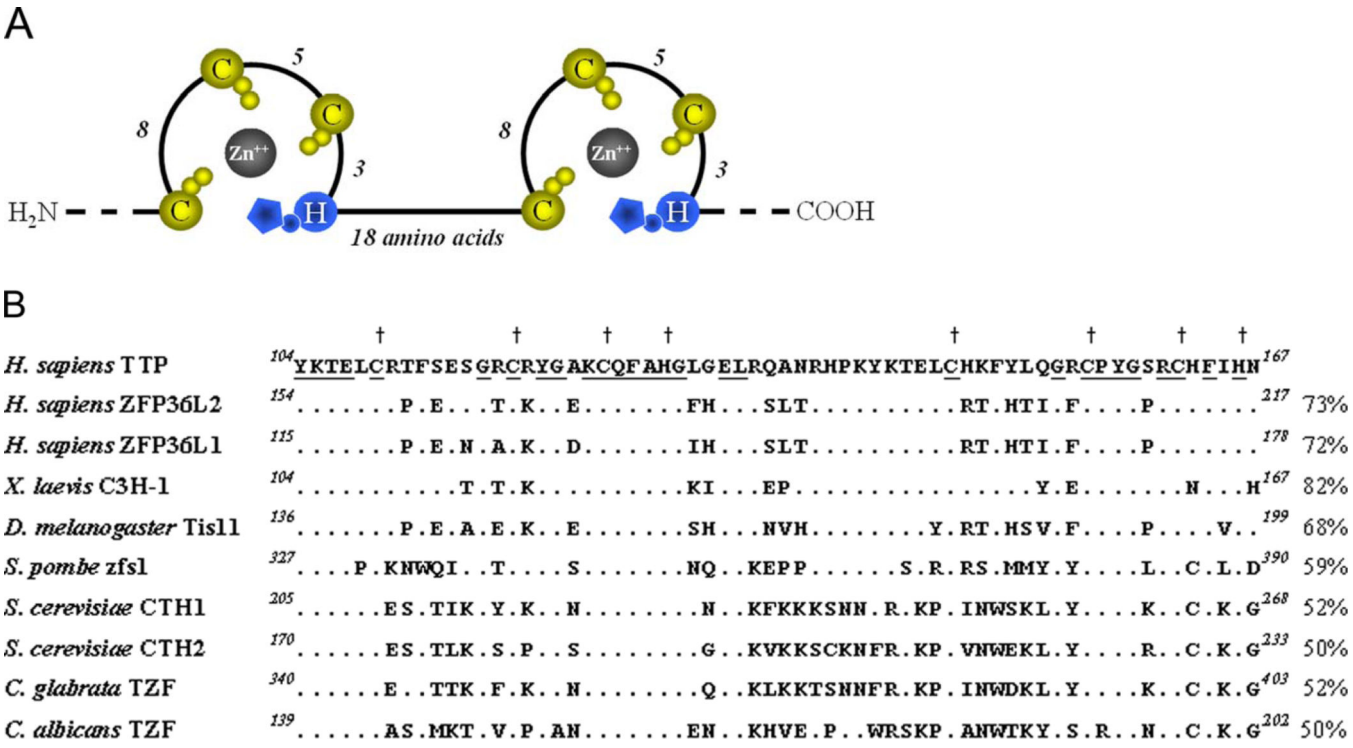

Figure 1.

Conservation of the TZF domain in eukaryotes. A is an illustration of the tandem CCCH motifs, separated by a spacer region of a conserved length, which constitute the conserved TTP-like, TZF domain. The numbers (8, 5 and 3) indicate the amino acid sequence length between the CCCH residues. In (B) is shown an alignment of several select TZF domain sequences from animals compared to those from yeasts (modified from Cuthbertson et al. 2007). Crosses above the alignment denote the conserved Cys and His residues that form the CCCH motifs. Identity with the top sequence (TTP) is indicated by dots in the aligned sequences. Numbers at the end of the sequences indicate the relative position of the TZF domain in the full-length protein. Percent identity with the TTP TZF domain is noted to the right of each sequence. NCBI accession numbers are as follows: *H. sapiens* TTP, NP_03398.1; *H. sapiens* ZFP36L2, NP_008818.3; *H. sapiens* ZFP36L1, NP_004917.2; *X. laevis* C3H–1, NP_001081885.1; *D. melanogaster* Tis11, NP_511141.2; *S. pombe* zfs1, CAB75997.1; *S. cerevisiae* CTH1, P47976; *S. cerevisiae* CTH2, P47977; *C. albicans* TZF, XP_717137.1; *C. glabrata* TZF, XP_445742.1.

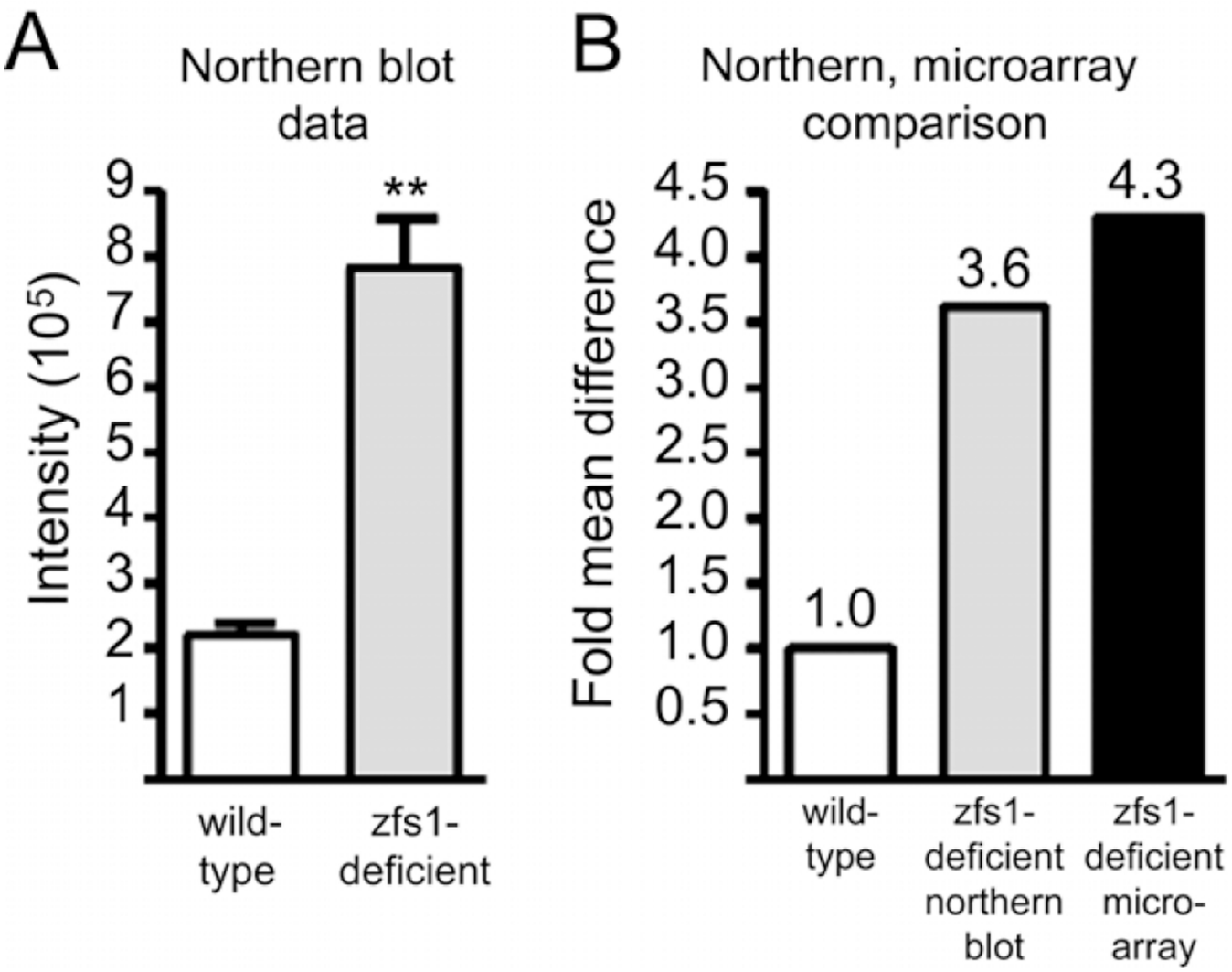

Figure 2.

Increased relative abundance of the *arz1* mRNA in the zfs1-deficient *S. pombe* strain. Northern analysis was used to confirm the results of the microarray comparison of expressed genes from wild-type (white bar) and zfs1-deficient (gray bar) *S. pombe* (modified from Cuthbertson et al. 2007), and a comparison of means of endogenous *arz1* mRNA levels from four paired samples is shown in (A). **, p=0.0012. Four independent steady state comparisons of expressed genes in wild-type and zfs1-deficient cells were carried out by microarray analyses, using Affymetrix Yeast 2.0 arrays. Fold mean difference of *arz1* mRNA levels is shown in (B), with levels in the wild-type strain set to 1.0 (white bar). The *arz1* mRNA was elevated by 4.3-fold in the zfs1-deficient strain as assessed by microarray (black bar) or by 3.6-fold in the zfs1-strain as assessed by northern analysis (gray bar).

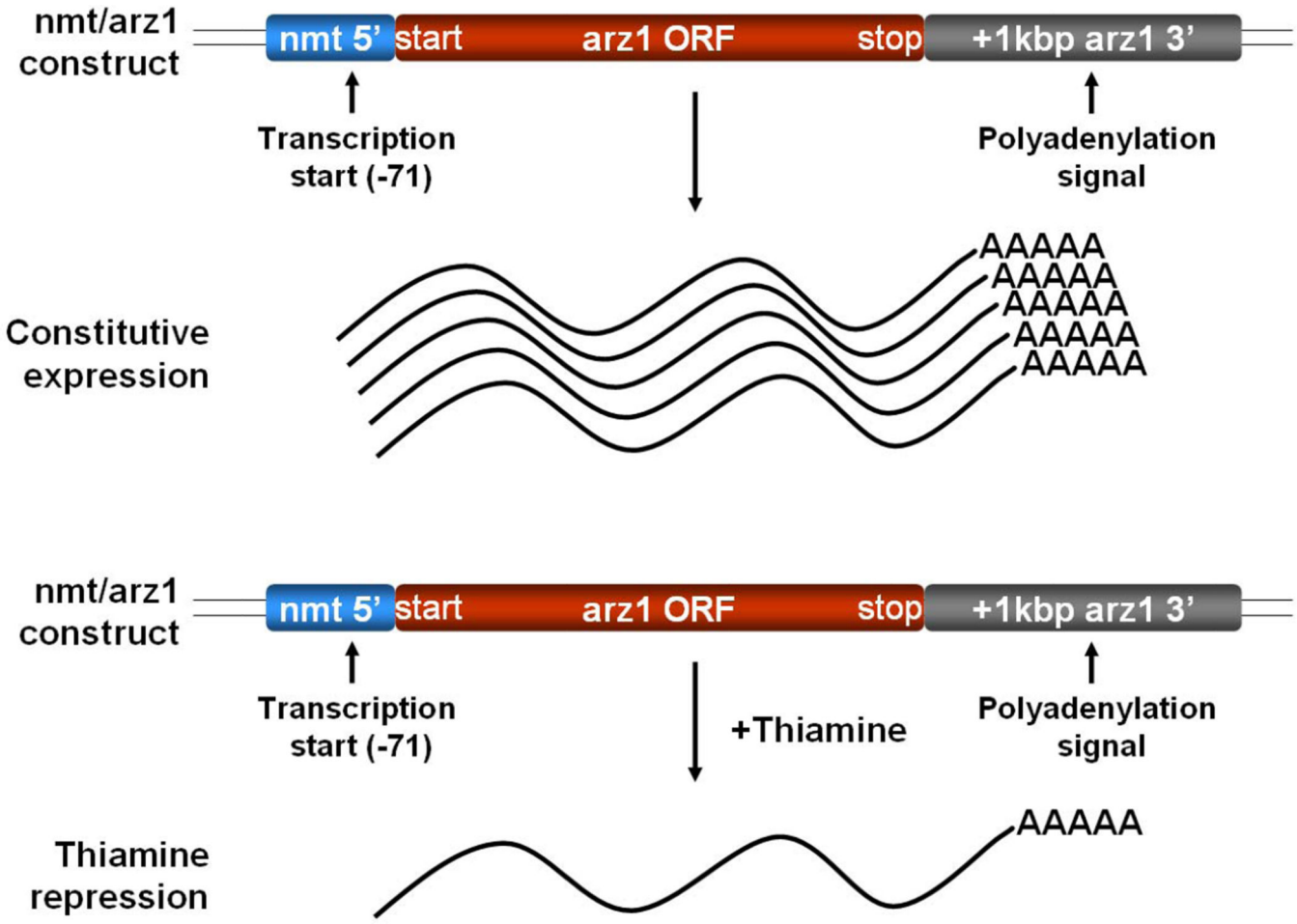

Figure 3.

The *nmt/arz1* expression construct is illustrated here. The *nmt* 5'-UTR is encoded by a 71 bp sequence extending from the start of transcription to the *arz1* start codon, and the *arz1* ORF (1479 bp) is followed by 1 kbp of downstream sequence. A predicted polyadenylation signal sequence is present at +1,918 b past the *arz1* start codon. Expression was repressed with 10 μM thiamine (final concentration) at the beginning of each time course. The *arz1* mRNA is depicted as wavy lines ending with a poly(A) tail.

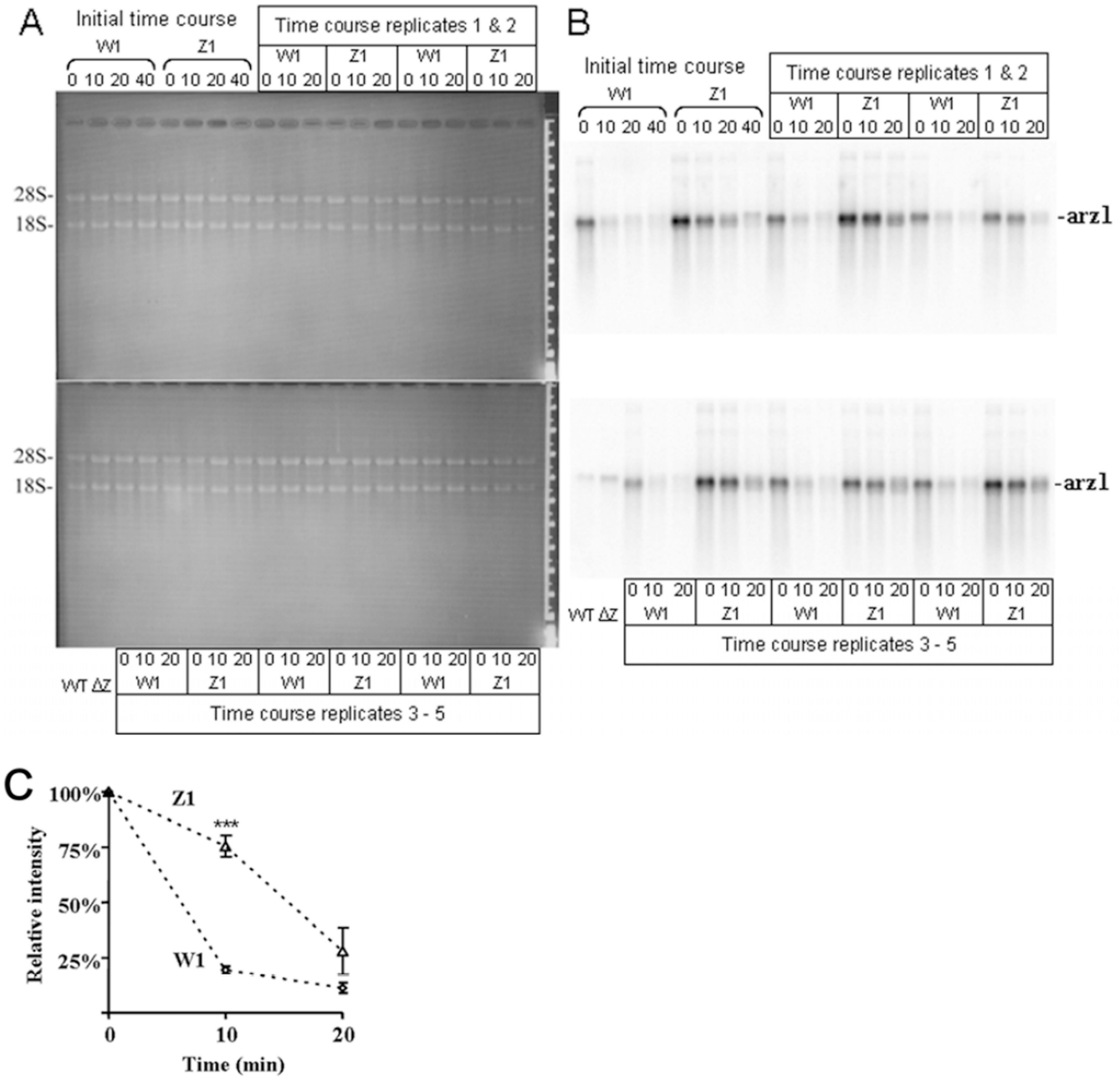

Figure 4.

Time courses of *arz1* mRNA repression by thiamine. W1 and Z1 represent the wild-type and zfs1-deficient strains transformed with the *nmt/arz1* construct, respectively (modified from Cuthbertson et al. 2007). In (A) is shown the ethidium bromide stained, UV illuminated 1.2% agarose gel of total cellular RNA (10 μg per lane) to illustrate loading consistency. In (B) is shown the corresponding northern blot probed with an *arz1*-specific probe. The *nmt* expressed *arz1* mRNA is calculated to be 1,989 b to the polyadenylation signal. Initial time courses were carried out to identify an appropriate time frame for quantitative comparisons, and one of these experiments is presented at the top left corner (A and B); W1 and Z1, 1–40 min. Replicate time courses for statistical comparison of means were limited to 0, 10 and 20

min samples (boxed labels in A and B) and these were used for the comparison of relative mean mRNA levels at 10 min shown in (C). WT and ΔZ labels indicate endogenous *arz1* mRNA levels in the wild-type and zfs1-deficient *S. pombe* strains, respectively.

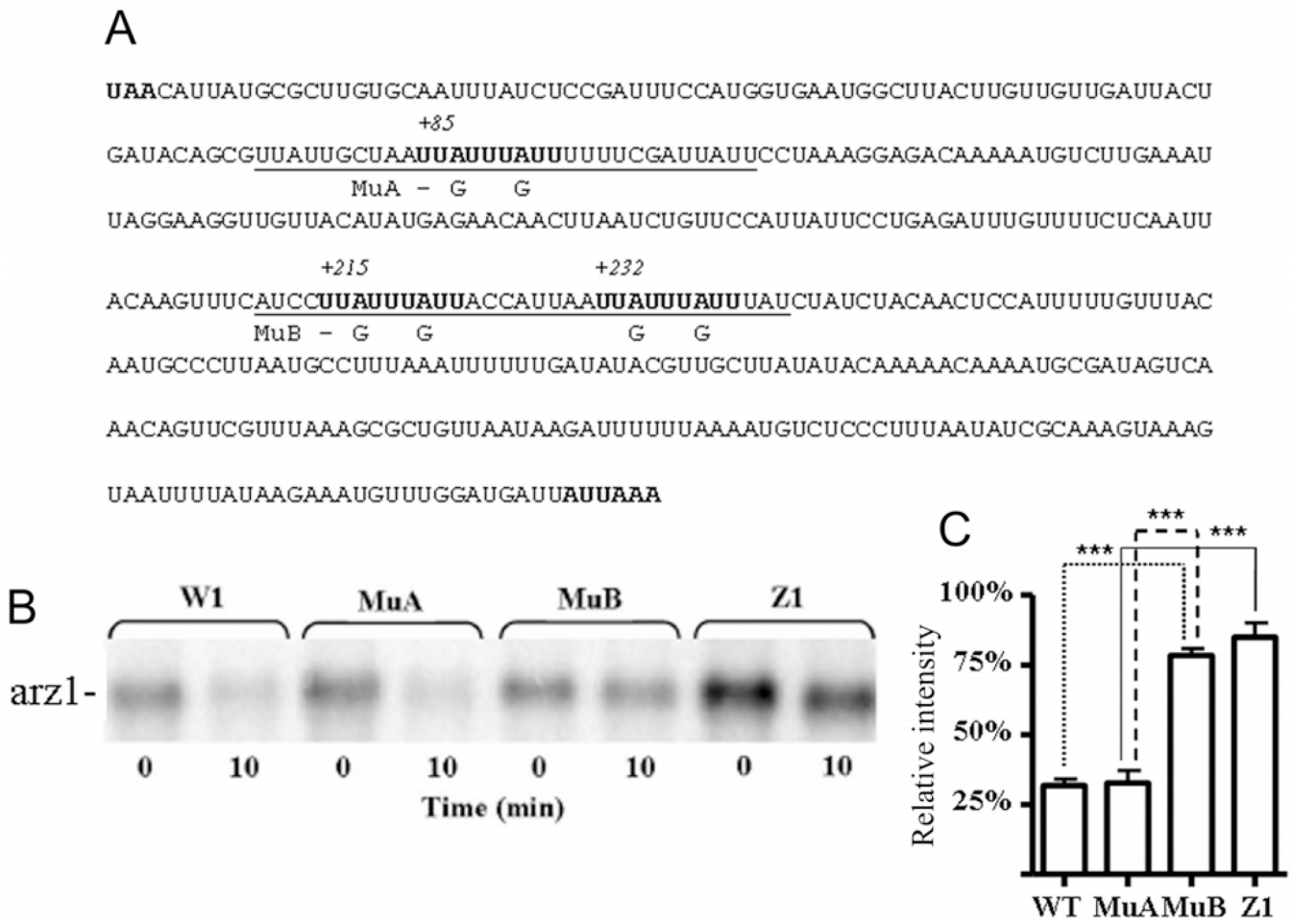

Figure 5.

Use of the *S. pombe* zfs1 system to evaluate the effects of mutations in the *arz1* transcript (from Cuthbertson et al. 2007). The sequence of the apparent *arz1* 3'UTR is presented in (A). This sequence contains two AU-rich elements (underlined) containing optimal TTP binding sites (UUAUUUAUU). AREa contains one binding site, beginning at 85 b past the stop codon (bold at beginning of sequence), and AREb contains two sites, beginning at 215 and 232 b past the stop codon. MuA and MuB are mutant *arz1* constructs, in which the adenosines in the binding sites are mutated in AREa or AREb, respectively. MuA contains two A to G mutations while MuB contains a total of four A to G mutations. MuA and MuB are wild-type *S. pombe* transformants with the respective *nmt/arz1* construct, while W1 and Z1 represent the same wild-type and zfs1-deficient strains transformed with un-mutated *nmt/arz1* as presented in Fig. 4. In (B) a representative northern blot is shown that compares W1, MuA, MuB and Z1 *arz1* mRNA levels at the time of thiamine addition (0 min) and 10 min after addition (10 min). Four independent samples of W1, MuA, MuB and Z1 are averaged in (C), and mean mRNA levels were compared for statistical significance by one way ANOVA (analysis of variance) using Bonferroni's correction for comparison of multiple means. All means were significantly different, with selected comparisons highlighted in (C) (***, $p<0.0001$).

Table I

PCR primers used in this study

Primer	Sequence (5' – 3')	Gene target	NCBI accession number	Target sequence position	Product length
F1	ATGACCGCTTCTGATACAGTCTAC	*arz1*	NC_003421.2	2,325,172–2,325,196	2,479 bp
R1	TTCGCAACGCTGGAAAGTTTGTGT			2,327,651–2,327,627	
F2	TTTCAATCTCATTCTCACTTTCTGA	*nmt/arz1*	pREP (Maundrell, 1993)	1098–1122	
R2	GGGCTCGATACTCTCGTGAATCC		NM_001023516.1	325–303	
F3	CTCTTGAACTCCTTAGGG	*arz1*	NM_001023516.1	98–115	665 bp
R3	TGCTATTAGAGTCGTCGG			763–746	
F4	TTGTTGACTGAGGCTCCTTTGAAC	*actin*	NM_001021513.1	310–333	801 bp
R4	AAACGATACCCAGGTCCGCTCTC			1111–1090	

Table II

Mutagenesis primers used in this study

Primer	Sequence (5' – 3')[a]	Gene target	NCBI accession number	Target sequence position
FMuB	CAAGTTTCATCCTT**G**TTT**G**TTACCATTAATT-**G**TTT**G**TTTATCTATC	*arz1*	NC_003421.2	2,326,853–2,326,898
RMuB	AGTTGTAGATAGATAAA**C**AAA**C**AATTAATGG-TAA**C**AAA**C**AAGGATG			2,326,905–2,326,860

[a] Bold residues in sequence indicate mutated base.